Insulin crystallization depends on zinc transporter ZnT8 expression, but is not required for normal glucose homeostasis in mice

K. Lemaire[a,1], M. A. Ravier[b,c,1], A. Schraenen[a], J. W. M. Creemers[d], R. Van de Plas[e], M. Granvik[a], L. Van Lommel[a], E. Waelkens[f], F. Chimienti[g], G. A. Rutter[h], P. Gilon[b], P. A. in't Veld[i], and F. C. Schuit[a,2]

[a]Gene Expression Unit, Department Molecular Cell Biology, Katholieke Universiteit Leuven, Herestraat 49, 3000 Leuven, Belgium; [b]Unit of Endocrinology and Metabolism, University of Louvain, Faculty of Medicine, Université Catholique de Louvain 55.30, 1200 Brussels, Belgium; [c]Institut National de la Santé et de la Recherche Médicale, U661, Equipe avenir, Centre National de la Recherche Scientifique, Unité Mixte de Recherche 5203, Université Montpellier (IFR3), Institut de Génomique Fonctionnelle, 34090 Montpellier, France; [d]Department of Human Genetics, Katholieke Universiteit Leuven, Herestraat 49, 3000 Leuven, Belgium; [e]Department of Electrical Engineering, Katholieke Universiteit Leuven, Kasteelpark Arenberg 10, 3001 Leuven, Belgium; [f]Prometa, Department of Molecular Cell Biology, Katholieke Universiteit Leuven, Herestraat 49, 3000 Leuven, Belgium; [g]Mellitech, SAS, Commissariat à l'Énergie Atomique, 17 rue des Martyrs, 38054 Grenoble, France; [h]Department of Cell Biology Division of Medicine Sir Alexander Fleming Building Imperial College, London Exhibition Road, London SW7 2AZ, United Kingdom; and [i]Department of Pathology, Vrije Universiteit Brussel, Laarbeeklaan 103, 1090 Brussels, Belgium

Edited by Donald F. Steiner, University of Chicago, Chicago, IL and approved July 16, 2009 (received for review June 15, 2009)

Zinc co-crystallizes with insulin in dense core secretory granules, but its role in insulin biosynthesis, storage and secretion is unknown. In this study we assessed the role of the zinc transporter ZnT8 using ZnT8-knockout (*ZnT8*$^{-/-}$) mice. Absence of ZnT8 expression caused loss of zinc release upon stimulation of exocytosis, but normal rates of insulin biosynthesis, normal insulin content and preserved glucose-induced insulin release. Ultrastructurally, mature dense core insulin granules were rare in *ZnT8*$^{-/-}$ beta cells and were replaced by immature, pale insulin "progranules," which were larger than in *ZnT8*$^{+/+}$ islets. When mice were fed a control diet, glucose tolerance and insulin sensitivity were normal. However, after high-fat diet feeding, the *ZnT8*$^{-/-}$ mice became glucose intolerant or diabetic, and islets became less responsive to glucose. Our data show that the ZnT8 transporter is essential for the formation of insulin crystals in beta cells, contributing to the packaging efficiency of stored insulin. Interaction between the *ZnT8*$^{-/-}$ genotype and diet to induce diabetes is a model for further studies of the mechanism of disease of human ZNT8 gene mutations.

dense core granule | diabetes | zinc

Zinc plays a crucial role in many cell functions; as a result, both zinc deficiency (1) and excess of free zinc (2) are toxic to mammalian cells. The abundance of zinc per cell is tissue-dependent and the zinc content of pancreatic beta cells is among the highest in the body. In beta cells, zinc was proposed to be required for multiple steps in insulin synthesis and release (3–5), but conclusive evidence is lacking. After synthesis in the ER, pro-insulin is transported into the Golgi apparatus where immature, pale secretory "progranules" are formed (6). These granules contain pro-insulin-zinc hexamers which are further processed into mature insulin and C-peptide by the prohormone convertases PC1/3 and PC2 (7). After maturation, the zinc-insulin hexamers form water-insoluble crystals (3). It has been suggested that crystal formation increases the degree of conversion of soluble pro-insulin to insoluble insulin, but nearly normal pro-insulin processing occurs in patients with mutated histidine-B10 insulin, which cannot crystallize (5). Futhermore, in several animal species such as guinea pig and hagfish, insulin does not have a histidine at position B10, so that no zinc-insulin crystals form; in these species, insulin is processed, and glucose homeostasis is normal (8, 9).

Two large zinc transporter families exist [reviewed in (10)]. Influx of zinc from the extracellular space into the cytosol is mediated by members of the, Slc39 (ZIP, Zrt/Irt-like protein) protein family, which has 14 isoforms. Efflux of zinc into the extracellular space as well as transport of zinc from the cytosol into intracellular organelles is mediated by 10 known isoforms of the Slc30 (ZnT, zinc transporters) family. Members of both transporter families exhibit tissue-specific expression, where they fulfil unique functions (10, 11). For example, ZnT8 (Slc30a8) was identified as a pancreatic beta cell-specific secretory granule zinc transporter (11, 12).

The interest in ZnT8 was aroused by the observation that epitopes of the ZnT8 protein are recognized by autoantibodies of patients with type 1 diabetes (T1D) (13). Furthermore, in a genome-wide association study (14), which was replicated in independent cohorts (15–18), an association was made between a SNP marker within the human SLC30A8 gene and genetic susceptibility to type 2 diabetes (T2D). The exact pathogenic significance of this polymorphism is still unknown.

To better understand the role of ZnT8 in pancreatic beta cells, we studied the phenotype of mice that are deficient in ZnT8 expression (*ZnT8*$^{-/-}$). Our data show that (*i*) ZnT8 is essential for insulin crystal formation that shapes the dense core of secretory granules, (*ii*) that ZnT8 is the only transporter in the beta cell that provides the required zinc ions for this process, and (*iii*) that ZnT8 is only essential for normal glucose homeostasis after the prolonged environmental β cell stress of a high fat diet.

Results

Islets from ZnT8$^{-/-}$ Mice Do Not Express the ZnT8 Protein, Have No Dithizone Staining, and Do Not Release Zinc. To assess the role of the beta cell zinc transporter ZnT8 in glucose homeostasis, we studied *ZnT8*$^{-/-}$ mice that were generated by Cre recombinase mediated deletion of the first exon, including the transcription start site (Fig. S1). Mice were born in Mendelian proportions and equal male/female ratio. No differences in growth and body weight were observed. *ZnT8*$^{-/-}$ mice did not express ZnT8 mRNA (Fig. 1*A*) and protein (Fig. 1*B*), and ZnT8 immunostaining of islet sections was negative (Fig. 1*C*). ZnT8 deficiency was not compensated by overexpression of one of the other zinc

Author contributions: K.L., M.A.R., P.G., and F.C.S. designed research; K.L., M.A.R., A.S., J.W.M.C., R.V.d.P., M.G., L.V.L., P.G., and P.A.i.V. performed research; E.W., F.C., and G.A.R. contributed new reagents/analytic tools; K.L., M.A.R., P.G., P.A.i.V., and F.C.S. analyzed data; and K.L. and F.C.S. wrote the paper.

The authors declare no conflict of interest.

This article is a PNAS Direct Submission.

[1]K.L. and M.A.R. contributed equally to this work.

[2]To whom correspondence should be addressed. E-mail: frans.schuit@med.kuleuven.be.

This article contains supporting information online at www.pnas.org/cgi/content/full/0906587106/DCSupplemental.

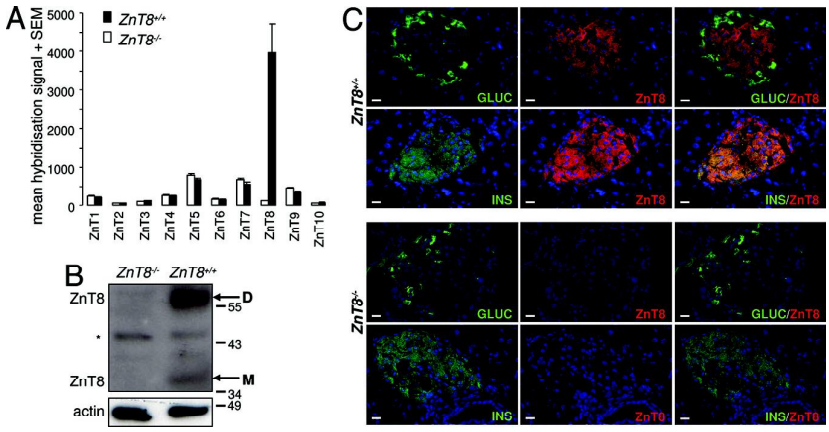

Fig. 1. ZnT8 expression is absent in *ZnT8*$^{-/-}$ mice. (*A*) mRNA expression of the 10 known efflux zinc transporters (Slc30a family) analyzed via microarray (n = 3). (*B*) ZnT8 protein expression was analyzed via western blots. Please note complete absence of the expected MW for ZnT8 monomers (M) and SDS-resistant dimers (D), * = non-specific protein. (*C*) Immunohistochemistry of pancreatic sections from *ZnT8*$^{-/-}$ and *ZnT8*$^{+/+}$ mice. In *ZnT8*$^{+/+}$ mice ZnT8 protein is strongly expressed in all insulin-positive cells and weakly expressed in a minority of glucagon cells. Nuclei are stained blue by 4′,6-diamidino-2-phenylindole (DAPI). (Scale bar, 10 μm.)

transporters (Fig. 1*A*). Furthermore, the mRNA expression profiles of *ZnT8*$^{-/-}$ and *ZnT8*$^{+/+}$ mice were very similar; as we found no differences in expression of mRNA's encoding other important beta-cell proteins (Fig. S2).

To investigate the consequence of beta-cell ZnT8 deficiency on islet zinc content, we performed in vivo and in vitro islet dithizone staining, a technique to distinguish pancreatic islets from exocrine cells (19), for instance used in vitro for human islet isolations (20) or in situ to visualise islets (21). *ZnT8*$^{-/-}$ islets were negative with this staining, both in situ (Fig. 2*A*), and in isolated islets (Fig. 2*B*). These results indicate that there is a direct connection between beta cell expression of the ZnT8 transporter, which allows zinc influx in insulin secretory granules and islet reactivity to dithizone.

Zinc release from secretory granules from small clusters of *ZnT8*$^{+/+}$ and *ZnT8*$^{-/-}$ islet cells stimulated by 15 mM glucose and 1 μM forskolin was imaged with total internal fluorescence microscopy (TIRF) using FluoZin-3 (22). A strong difference between *ZnT8*$^{+/+}$ and *ZnT8*$^{-/-}$ beta cells was found (6.3 $\pm$ 1.1 vs. 0.07 $\pm$ 0.03 zinc exocytotic events/min, respectively, $P <$ 0.0001) (Fig. 2*C* and *D*). A general defect of exocytosis in *ZnT8*$^{-/-}$ beta cells was excluded by measuring release of NPY-

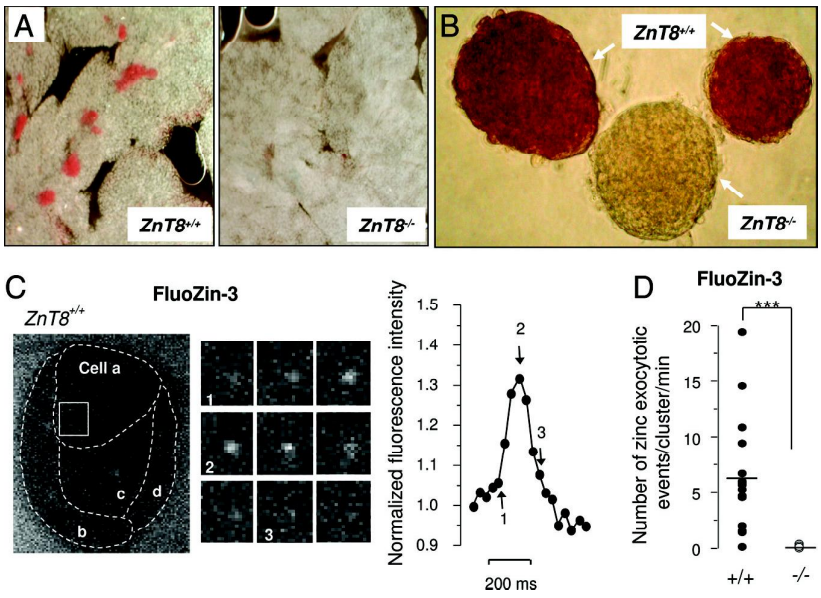

Fig. 2. ZnT8 is required for islet dithizone staining and glucose-regulated granular zinc release from beta cells. (*A*) Dithizone staining of pancreata from *ZnT8*$^{+/+}$ and *ZnT8*$^{-/-}$ mice, 15 min after i.p. injection of the dye. Islets can be seen at the pancreatic surface of *ZnT8*$^{+/+}$ mice but not of *ZnT8*$^{-/-}$ mice. (*B*) Dithizone staining of isolated islets is positive in *ZnT8*$^{+/+}$ mice (red color) but negative in *ZnT8*$^{-/-}$ mice. (*C*) Zinc release from clusters of islet cells imaged by TIRF microscopy during 7 min. Cluster size was 3.7 $\pm$ 0.4 vs. 3.8 $\pm$ 0.3 cells, for *ZnT8*$^{+/+}$ and *ZnT8*$^{-/-}$, respectively (ns). Medium contained 8 μM FluoZin-3 and exocytosis was stimulated by 15 mM glucose and 1 μM forskolin. One zinc exocytotic event from a *ZnT8*$^{+/+}$ four-cell cluster is illustrated, boundaries between cells are shown as dotted lines (left panel). Images were taken every 30 ms in the region delimited by a square (middle panel), and the intensity of fluorescence for this release event is plotted on the right panel. Arrows show fluorescence intensity for the indicated time points illustrated in the middle panel, (*D*) Quantification of zinc exocytotic events in clusters of *ZnT8*$^{+/+}$ and *ZnT8*$^{-/-}$ islet cells. The horizontal line shows the average of 18 clusters from three individual mice.

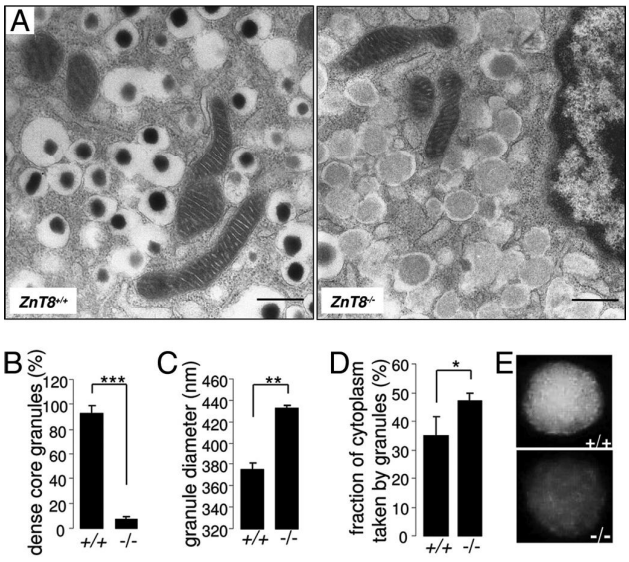

Fig. 3. ZnT8 is required for zinc-insulin crystal formation. (*A*) Transmission electron microscopy of representative $ZnT8^{+/+}$ and $ZnT8^{-/-}$ beta cells ($ZnT8^{+/+}$, $n = 4$; $ZnT8^{-/-}$, $n = 7$). Secretory granules of $ZnT8^{-/-}$ beta cells lack the electron dense cores and halo that are typical for wild-type mice. Furthermore, the size of the secretory granules is larger in $ZnT8^{-/-}$ mice. (Scale bar, 0.5 μm.) (*B*) Quantification of % dense core granules in $ZnT8^{+/+}$ and $ZnT8^{-/-}$ beta cells (n = 622 and 740 granules, respectively,), (*C* and *D*) Morphometric quantification of granule diameter (n = 126 and 83 granules, respectively), (*C*) and relative cytoplasmic volume of the granule pool (*D*) in $ZnT8^{+/+}$ and $ZnT8^{-/-}$ beta cells. Data are mean ± SEM, statistical analysis via unpaired Student's t test: *, $P < 0.05$; **, $P < 0.001$; ***, $P < 0.0001$. (*E*) Bright light reflection of islolated $ZnT8^{+/+}$ islets contrasts with dull gray appearance of $ZnT8^{-/-}$ islets under a dissection microscope.

pHluorin, a pH sensitive probe (23) (Fig. S3 *A* and *B*) and by insulin release experiments (see following paragraph).

Replacement of Dense Core Secretory Granules in Beta Cells by Pale "Progranules" in Islets of ZnT8$^{-/-}$ Mice. Because zinc influx in secretory granules should precede formation of zinc-insulin crystals, we next compared via transmission electron microscopy the ultrastructure of $ZnT8^{+/+}$ and $ZnT8^{-/-}$ beta cells. In control beta cells, most (>90%) secretory granules contained a typical dense core that is composed of zinc-insulin crystals (Fig. 3*A*, *Left*). In contrast, more than 90% of all secretory granules in beta cells from $ZnT8^{-/-}$ mice had lost this condensed aspect and were completely filled with pale looking proteinaceous material (Fig. 3*A*, *Right*). Quantitatively, there was an almost all or none phenotypic difference between the two mouse strains (Fig. 3*B*). Furthermore, the mean diameter of the secretory granule was significantly larger in $ZnT8^{-/-}$ mice than in $ZnT8^{+/+}$ mice (Fig. 3*C*) so that the calculated secretory granule pool occupied a 12% larger fractional cell volume in $ZnT8^{-/-}$ mice (Fig. 3*D*). These data show that ZnT8 is essential for zinc influx and zinc-insulin crystal formation. We further noted that the loss of dense core granules was correlated to loss of light reflection of isolated islets (Fig. 3*E*). While normal islets can be easily recognized in pancreatic digest because they appear brightly white $ZnT8^{-/-}$ islets were dull greyish. We conclude that expression of ZnT8 transporters allows growth of zinc-insulin microcrystals in secretory granules shaping the ultrastructure dense cores and explaining bright light reflection of isolated islets.

Insulin Processing Is Not Affected in ZnT8$^{-/-}$ Mice. To exclude that the enrichment of pale granules in $ZnT8^{-/-}$ mice was the result

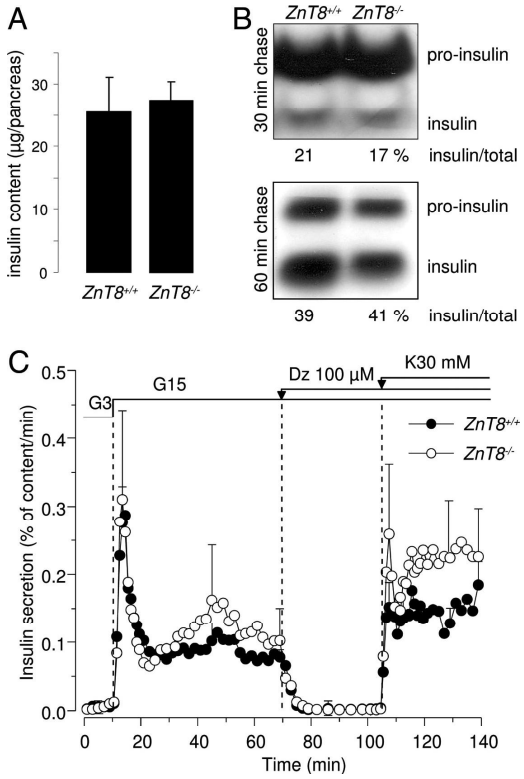

Fig. 4. Insulin biosynthesis, processing and release are not affected in $ZnT8^{-/-}$ mice. (*A*) Insulin content from isolated pancreata of $ZnT8^{-/-}$ and $ZnT8^{+/+}$ mice. Data are mean ± SEM, $n = 4$). (*B*) Radiometric quantification of pro-insulin synthesis and conversion to insulin. Isolated islets from $ZnT8^{-/-}$ and $ZnT8^{+/+}$ mice were labeled for 30 min with ^{35}S-amino acids and chased for 30 min (upper panel) or 1 h (lower panel) in the presence of 10 mM glucose. Radioactive (pro)-insulin was quantified after immunoprecipitation, gel electrophoresis and autoradiography. Similar amounts of pro-insulin synthesis and conversion were found [30 min (≈20%) and 1 h (≈40%), ($n = 3$)] in both strains. (*C*) Glucose-induced insulin release. After overnight culture in 10 mM glucose (G), islets from adult $ZnT8^{+/+}$ (black circle) and $ZnT8^{-/-}$ (open circle) mice were perifused for 30 min with a medium containing 3 mM glucose. When indicated by the arrows, the glucose concentration was increased to 15 mM, the K_{ATP} channel opener diazoxide (Dz) was added, and the KCl concentration was increased from 4.8 to 30 mM. Data are mean ± SEM of four experiments.

of severely delayed pro-hormone processing, we performed three different experiments, each indicating that pro-insulin conversion to insulin is normal in $ZnT8^{-/-}$ mice. First, total pancreatic immunoreactive (pro-)insulin content was the same in $ZnT8^{-/-}$ and $ZnT8^{+/+}$ mice (Fig. 4*A*). Second, isolated islets from $ZnT8^{+/+}$ and $ZnT8^{-/-}$ mice were labeled for 30 min with [^{35}S]methionine/cysteine and chased for 30 min or 1 h at 10 mM glucose, followed by quantification of newly synthesized pro-insulin and insulin (Fig. 4*B*). Compatible with normal processing kinetics, beta cells from both $ZnT8^{-/-}$ and $ZnT8^{+/+}$ mice had processed the same amount of newly synthesized pro-insulin to insulin during this chase period (Fig. 4*B*). Third, using in situ mass spectral tissue profiling (24), we found that abundance of both mature processed insulin and mature glucagon was the same in $ZnT8^{-/-}$ and $ZnT8^{+/+}$ islets (Fig. S4).

Glucose-Induced Insulin Release and Calcium Changes Are Normal in ZnT8$^{-/-}$ Mice. We next investigated whether the lack of insulin crystals had functional consequences at the level of glucose-induced insulin release. Because the water soluble pharmaceu-

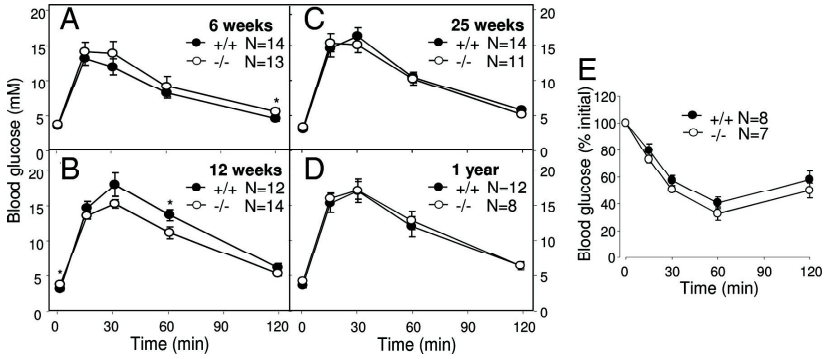

Fig. 5. Glucose and insulin tolerance in *ZnT8*$^{+/+}$ and *ZnT8*$^{-/-}$ mice fed a control diet. *ZnT8*$^{+/+}$ (black circles) and *ZnT8*$^{-/-}$ (open circles) mice were given a control chow and were tested between 6 and 52 weeks of age. Blood glucose levels were measured at the indicated time points after i.p. injection of 2.5 mg glucose/g BW glucose in overnight (16 h) fasted mice aged 6 weeks (*A*), 12 weeks (*B*), 25 weeks (*C*), and 1 year (*D*). (*E*) Insulin tolerance test after injection of 0.75 mU/g BW insulin i.p. in 6 h fasted mice aged 12 weeks, expressed as % over baseline. Data are mean ± SEM, statistical analysis via unpaired Student's *t* test: *, $P \leq 0.05$.

tical form of insulin is known to act more rapidly than zinc-crystalline preparations, it was conceivable that different kinetics of insulin release would exist between *ZnT8*$^{-/-}$ and *ZnT8*$^{+/+}$ mice. However, as is illustrated by perifusion experiments from *ZnT8*$^{-/-}$ and *ZnT8*$^{+/+}$ islets (Fig. 4*C*), no difference in insulin release after glucose or KCl stimulation could be seen. This indicates that zinc-insulin crystals do not impose a significant delay on the rate of insulin exocytosis and/or diffusion of interstitial hormone into the circulation, at least in the tested conditions. Zinc was also proposed to alter cytosolic Ca^{2+} concentration ($[Ca^{2+}]_c$) in beta cells (25, 26) but we found no difference in $[Ca^{2+}]_c$ of *ZnT8*$^{-/-}$ and *ZnT8*$^{+/+}$ islets (Fig. S5), and we detected no difference in amplitude or frequency of oscillations. In summary, we show that ZnT8-deficiency per se does not affect glucose stimulated insulin release.

Diet-Dependent Induction of Glucose Intolerance in ZnT8$^{-/-}$ Mice. To assess the whole animal metabolic consequence of beta-cell ZnT8 deficiency, we measured basal blood glucose and insulin levels as well as glucose tolerance after i.p. injection of glucose in *ZnT8*$^{-/-}$ and *ZnT8*$^{+/+}$ mice. In both sexes, random fed and fasting blood glucose levels were the same in both mouse strains when tested at age 12 and 25 weeks (Table S1). Furthermore, plasma insulin and glucagon levels were similar in *ZnT8*$^{-/-}$ and *ZnT8*$^{+/+}$ mice (Table S2). When given a regular diet, glucose tolerance was the same in *ZnT8*$^{-/-}$ and *ZnT8*$^{+/+}$ mice studied at age 6 weeks (Fig. 5*A*), 12 weeks (Fig. 5*B*), 25 weeks (Fig. 5*C*), and 1 year (Fig. 5*D*). Furthermore, no difference in insulin sensitivity was observed between *ZnT8*$^{+/+}$ and *ZnT8*$^{-/-}$ mice at the age of 12 weeks (Fig. 5*E*). Figs. S6 and S7 show glucose tolerance for males and females separately. In contrast, glucose homeostasis deteriorated in *ZnT8*$^{-/-}$ mice upon prolonged feeding a high-fat diet (HFD). This regimen resulted in 10% larger weight gain in *ZnT8*$^{-/-}$ mice and a mild degree of glucose intolerance measured after 10 weeks (Fig. S8). With longer exposure to HFD, this difference deteriorated to overt diabetes (blood glucose level >14 mM) in half of the *ZnT8*$^{-/-}$ mice, while under the same conditions all of the control mice remained non-diabetic ($P <$ 0.05—Fig. S8*B*). Two arguments support that β cell dysfunction is the cause for decompensation of glucose homeostasis: (*i*) islets of *ZnT8*$^{-/-}$ mice fed a HFD for 16 weeks lost part of glucose stimulated insulin release as compared to *ZnT8*$^{+/+}$ islets (Fig. S8*E*), and (*ii*) insulin sensitivity remained normal (Fig. S8*D*).

Together, these data indicate that loss of ZnT8 expression in *ZnT8*$^{-/-}$ beta cells is well-tolerated when given a normal diet, but that beta cells fail, causing diabetes in some animals after prolonged HFD.

Discussion

Our study of *ZnT8*$^{-/-}$ mice provides results with respect to the role of ZnT8 and zinc in beta-cell biology. The most striking phenotypic changes in *ZnT8*$^{-/-}$ mice are (1) complete loss of islet dithizone staining, (2) loss of zinc release from secretory granules, (3) presence of pale "progranules" instead of dense-core granules that occupy a larger relative secretory granule volume, (4) normal glucose tolerance and adequate beta-cell function under standard laboratory conditions, and (5) failure of beta cells to maintain glucose homeostasis under the prolonged metabolic stress of a high-fat diet.

Our data strongly suggest that dithizone (27) stains islets red because of the presence of beta-cell zinc-insulin crystals. The exact reason for this intense staining reaction is unknown, but it is possible that the steric position of the two zinc ions in the crystal structure allows specific binding of the dye. Since *ZnT8*$^{-/-}$ beta cells do not secrete zinc after glucose/forskolin stimulation and since the other zinc transporters are expressed normally, our data indicate that ZnT8 is the only zinc transporter that can import zinc into the secretory granules for insulin crystal formation. Pale beta-cell secretory "progranules" were previously found to be enriched in biosynthetically active beta cells and proposed to be filled with unprocessed, non-crystalline pro-insulin (6, 28). Radiometric analysis of pro-insulin synthesis and in situ peptidomics of islets in *ZnT8*$^{+/+}$ and *ZnT8*$^{-/-}$ mice make it unlikely that *ZnT8*-deficiency leads to immature granules because of a severe delay in pro-insulin processing. In fact, our data suggest that even when secretory granule zinc content is strongly reduced, proinsulin processing occurs normally. In agreement with this idea, normal insulin conversion occurs in guinea pig and hagfish, while at the same time beta cells in these species can form no zinc-insulin crystal (8, 9). The abundance of intact 5,800 Da insulin peptide as one sharp mass peak in the spectrum of islets of both *ZnT8*$^{-/-}$ and *ZnT8*$^{+/+}$ mice excludes the possibility that zinc plays a major role in protecting cellular insulin stores from degradation. The lack of insulin crystal formation probably is the reason for the increased vesicle diameter, since soluble insulin can act as an osmolite. As equal amounts of insulin are stored in wild-type and knockout pancreata, it is predicted that a larger volume percentage of the beta cell is taken by the granule pool. This idea is supported by the measurement of the relative surface area occupied by secretory granules, which is significantly increased in the *ZnT8*$^{-/-}$ mice.

We further show that insulin release (both time kinetics and the percent released per beta cell per hour) is well preserved in the absence of insulin crystals, meaning that dissolving insulin crystals in the islet interstitium does not delay the rate at which

insulin enters the circulation. Furthermore, *ZnT8*$^{-/-}$ mice have normal pancreatic insulin content and unaltered insulin synthesis. Together with normal insulin sensitivity, these data explain the complete normal glucose tolerance of *ZnT8*$^{-/-}$ when fed a normal diet. We extensively tested animals for glucose tolerance and in both sexes up to 1 year of age and found no abnormalities. It should be noted, however, that in a separate London colony of ZnT8$^{-/-}$ mice (29), studied in parallel with our colony, impaired glucose tolerance was observed with standard diet, despite the existence of less dramatic alterations in granule morphology. Since the Leuven and London colonies were derived from the same mouse line, we wondered whether subtle changes in the environment could be responsible for differences in phenotype. To address this issue, we fed control animals and *ZnT8*$^{-/-}$ mice a HFD, a condition known to increase the metabolic demand for insulin and which can trigger beta- cell failure in the presence of an underlying genetic defect (30, 31). In agreement with this idea, we observed progressive deterioration of glucose homeostasis with time in the knockout strain. This decompensation is explained by abnormal beta-cell function as insulin sensitivity remained normal, while glucose stimulation of insulin release from isolated islets diminished. Other murine models exist in which a combination of genetic predisposition and environmental stress of HFD is required to trigger beta cell decompensation (30). In the case of the heterozygous mutation of the phosphorylation site (Ser51Ala) of the translation initiation factor eIF2alpha, high fat diet triggers decompensation of the unfolded protein response with ER dilation and poor conversion of proinsulin to insulin (31). In the *ZnT8*$^{-/-}$ strain, it is conceivable that impaired granule packaging in beta cells that cannot form insulin crystals leads to secretory failure when the metabolic insulin demand is high. Our data are in agreement with the genetic screens in human subjects where polymorphisms in the SLC30A8 gene were detected in models of complex, multifactorial disease, rather than in monogenic forms of type 2 diabetes. Also in agreement with our own data, an independent *ZnT8*$^{-/-}$ line was reported recently in which normal glucose tolerance was observed when the animals were given a standard diet (32); in these animals islet zinc content decreased dramatically, but insulin crystals were not measured; moreover, the influence of HFD was not tested.

Recently, the hypothesis was proposed that Zn^{2+}, co-released with insulin, inhibits glucagon secretion in a paracrine manner (33). Since glucose stimulated zinc release is diminished in islets from *ZnT8*$^{-/-}$ mice, it is conceivable that the mechanism of impaired glucose homeostasis is based upon derepression of the alpha cell rather than failure of glucose-stimulated insulin release from beta cells when glucose intolerance arises. Two arguments are against this idea. First, we found no significant rise in plasma glucagon levels in *ZnT8*$^{-/-}$ mice. Second, Nicolson et al. observed that glucose suppression of glucagon release from isolated *ZnT8*$^{-/-}$ islets was well preserved (29). Further work is needed to examine the possibility that small amounts of free zinc, co-secreted with soluble insulin, is still sufficient to inhibit alpha cell activity.

In summary, this study shows on the one hand that the ZnT8 transporter is absolutely essential for the formation of insulin crystals, but on the other hand that insulin crystallization per se is not required for normal glucose homeostasis in mice. The in vivo data suggest that zinc-insulin crystals allow a better insulin packaging efficiency in beta-cell granule stores, which seems relevant for resisting abnormal glucose homeostasis under the metabolic stress of a prolonged high fat diet. Since type 2 diabetes is a complex multifactorial disease, where genetic predisposition interacts with environmental factors, we believe that the mouse model described in the present paper may be of interest to further study the precise chain of events that occur in patients with ZNT8 gene mutations.

Materials and Methods

Generation of ZnT8$^{-/-}$ Mice, Breeding, and Genotyping. All procedures involving mouse tissues were conducted according to guidelines approved by the K.U.Leuven animal welfare committee. The strategy to generate *ZnT8*$^{-/-}$ mice is summarized in Fig. S1. This procedure, performed by genOway, involved insertion of LoxP sites with a neomycin selection cassette upstream of exon 1 and within intron 1 of the gene. After homologous recombination in SV129-derived ES cells, and injection of recombinant cells into C57BL/6 blastocytes, the floxed mice were mated with CMV-Cre-expressing C57BL/6J mice to generate heterozygous mice carrying the *ZnT8*$^{-/-}$ allele. These mice were then crossed with WT C57Bl6/J (Janvier) to generate heterozygous ZnT8$^{+/-}$ mice which were bred to obtain homozygous male and female *ZnT8*$^{+/+}$ and *ZnT8*$^{-/-}$ mice that were used for all experiments in this study. Mice were fed a normal diet (ssniff) or a HFD (Research Diets). The genotype of the mice was checked via PCR using primer MEL1-L2/F4 5′-GTCTTGTGTGCTGGATGTATGG/5′-CTCTGCTTGGAAATACCCAGTCTCC.

Isolation of Mouse Pancreatic Islets. Islets were isolated by injection of collagenase P (Roche) in the pancreatic duct followed by 3-min digestion at 37 °C, and dispersion by pipetting. Islets were hand-picked in HEPES Krebs buffer (20 mM HEPES, pH 7.4; 119 mM NaCl; 4.75 mM KCl; 2.54 mM $CaCl_2$; 1.2 mM $MgSO_4$; 1.18 mM KH_2PO_4; 5 mM $NaHCO_3$) containing 5 mM glucose and 0.5% BSA. Islet light microscopic brightness was evaluated with a cold light source (3,000 K) using a dissection microscope.

Zinc Transporter Gene Expression Analysis. Total *RNA* from mouse islets was extracted using the Absolutely RNA microprep (Stratagene) and was used to analyze mRNA expression via mouse Gene 1.0 ST arrays according to manufacturer's manual 701880Rev4 (Affymetrix) (for detailed method see *SI Text*). Total protein extracts were obtained from freshly isolated islets which were lysed in S1 extraction buffer (50 mM Tris, pH 8; 1% Nonidet P-40; 150 mM NaCl; 1 mM EDTA). Protein extracts were separated by 4–12% SDS/PAGE (Invitrogen). ZnT8 antibody (Mellitech) and beta-actin antibody (Abcam) were used for immunodetection.

Zinc Staining with Dithizone. Dithizone staining was performed with a 0.13 mM dithizone solution in PBS for 5 min at room temperature for isolated islets or 15 min after i.p. injection [500 μL dithizone solution (10 mg/mL)] for in situ staining (34).

Measurment of Zinc Release via TIRF. Small clusters of islet cells from *ZnT8*$^{+/+}$ and *ZnT8*$^{-/-}$ mice were plated on coverslips 2 days before imaging. Experiments were performed at 37 °C as previously described (35). FluoZin-3 (Molecular Probes) was used at a final concentration of 8 μmol/L. Exocytosis was measured using a Nikon objective lens (Apo, 60×, numerical aperture = 1.49, infinity corrected) mounted on a Nikon Eclipse TE2000-E inverted microscope, using laser light of 491 nm excitation (Mag Biosystems) and 535 nm emission. Images were collected every 30 ms with a 30 ms-exposure during 7 min using a charge coupled device camera (Quantem, Roper Scientific) and MetaFluor software (Molecular Devices).

Islet ZnT8 Immunostaining and Beta Cell Ultrastructure. ZnT8 immunostaining was performed on 6-μm cryosections of snap-frozen pancreata from *ZnT8*$^{+/+}$ and *ZnT8*$^{-/-}$ mice that were 4% formalin fixed and incubated with rabbit anti ZnT8 (Mellitech), guinea pig anti insulin (a gift of Dr. C. Van Schravendijk, Brussels, Belgium), mouse anti glucagon (Novo). Binding of primary antibodies was visualized with anti-rabbit Cy3, anti- mouse fluorescein isothiocyanate or anti-guinea pig isothiocyanate (Jackson Immunoresearch) and examined in a fluorescence microscope (Nikon) equipped with an Orca AG camera (Hamamatsu) and NIS-elements imaging software (Nikon). Controls included the use of primary antibodies absorbed with the antigen against which the antibody was raised. Beta cell ultra-structure was evaluated in intact pancreas immersion-fixed in 2.5% glutaraldehyde in 0.1 M sodium cacodylate buffer (pH 7.4), postfixed in 1% osmium tetroxide, stained with 2% uranyl acetate and embedded in Spurr's resin. Ultrathin plastic sections from *ZnT8*$^{+/+}$ and *ZnT8*$^{-/-}$ pancreas were examined in a Tecnai 10 electron microscope (FEI).

In Situ Proteomics. Cryosections (10 μm) of pancreatic tissue were mounted on MALDI-MS compatible glass slides with a conductive coating (Bruker Daltonics). Tissue was covered with matrix solution (alpha-cyano-4hydroxy-cinnamic acid 7 mg/ml in acetonitrile 50%, 0.05% TFA) using a dedicated nanodrop spotter (Portrait P630, Labcyte Inc.). MALDI mass profiling of the islets was performed by direct mass spectral measurement using an ABI 4800 MALDI

TOF/TOF Analyzer (Applied Biosystems) running in linear mode. The selected mass over charge (m/z) range was 2,000–17,000 (24).

Measurement of Pro-Insulin Biosynthesis, Insulin Secretion, and Dynamics of $[Ca^{2+}]_c$. Insulin biosynthesis was performed as described earlier (31), with minor changes see *SI Text*. Insulin release was measured as described before (35, 36) in batches of 25 overnight cultured *ZnT8*$^{+/+}$ and *ZnT8*$^{-/-}$ islets perifused at 37 °C with test solutions of which the composition is indicated at the top of the figure. At the end of the experiments, the islets were recovered, and their insulin content was determined after extraction in acid-ethanol. Cytosolic calcium was measured as described before (37) in overnight cultured *ZnT8*$^{+/+}$ and *ZnT8*$^{-/-}$ islets loaded at 37 °C for 2 h with 2 μmol/L fura PE3-AM (MoBiTec).

Glucose/Insulin Tolerance Tests and Insulin/Glucagon Assays. For the glucose tolerance tests, mice of 6, 12, and 25 weeks of age were fasted overnight (16 h). Glucose (2.5 mg/g BW) was administered i.p. and blood glucose levels were followed during 2 h using AccuCheck glucostrips. For insulin tolerance test, 6-h fasted mice were injected i.p. with insulin (0.75 mU/g BW) and blood glucose levels were measured as described above. Plasma insulin was measured from blood taken via the vena cava or the tail vein and centrifuged for 10 min at 1,100 $\times$ g at 4 °C. For glucagon measurements, aprotinin (250 IU/μL) was added to blood before centrifugation. Insulin content was measured in the total pancreas after dissection, snap freezing in liquid nitrogen, and homogenization in 75% ethanol; 0.1% Triton-X-100; 1.2% 12 N HCl using a Douncer. (Pro-)insulin was quantified using ELISA (Crystal Chem) and glucagon was quantified using RIA (Linco).

ACKNOWLEDGMENTS. We thank Marleen Bergmans, Nicole Buelens, and Julien Carpent for excellent technical assistance and D. Daro for help constructing the adenovirus expressing pHluorin. This work was supported by postdoctoral fellowships from the FWO Vlaanderen to K.L., and from the FNRS, Brussels to M.A.R. Research was further supported by grants of the European Union (EURODIA FP6–518153), the Belgian Ministry for Science Policy (IUAP P6/40), SymBioSys (the K.U. Leuven center of excellence of Systems Biology), the K.U. Leuven (GOA 2004/11 and GOA 2008/16), and ARC (05/10–328) from the General Direction of Scientific Research of the French Community of Belgium. P.G. is research director from the FNRS, Brussels.

1. Sekler I, Sensi SL, Hershfinkel M, Silverman WF (2007) Mechanism and regulation of cellular zinc transport. *Mol Med* 13:337–343.
2. Frederickson CJ, Koh JY, Bush AI (2005) The neurobiology of zinc in health and disease. *Nat Rev Neurosci* 6:449–462.
3. Dodson G, Steiner D (1998) The role of assembly in insulin's biosynthesis. *Curr Opin Struct Biol* 8:189–194.
4. Huang XF, Arvan P (1995) Intracellular transport of proinsulin in pancreatic beta-cells. Structural maturation probed by disulfide accessibility. *J Biol Chem* 270:20417–20423.
5. Carroll RJ, et al. (1988) A mutant human proinsulin is secreted from islets of Langerhans in increased amounts via an unregulated pathway. *Proc Natl Acad Sci USA* 85:8943–8947.
6. Orci L, et al. (1985) Direct identification of prohormone conversion site in insulin-secreting cells. *Cell* 42:671–681.
7. Creemers JW, Jackson RS, Hutton JC (1998) Molecular and cellular regulation of prohormone processing *Semin Cell Dev Biol* 9:3–10.
8. Emdin SO, Dodson GG, Cutfield JM, Cutfield SM (1980) Role of zinc in insulin biosynthesis. Some possible zinc-insulin interactions in the pancreatic B-cell. *Diabetologia* 19:174–182.
9. Smith LF (1966) Species variation in the amino acid sequence of insulin. *Am J Med* 40:662–666.
10. Liuzzi JP, Cousins RJ (2004) Mammalian zinc transporters. *Annu Rev Nutr* 24:151–172.
11. Chimienti F, Devergnas S, Favier A, Seve M (2004) Identification and cloning of a beta-cell-specific zinc transporter, ZnT-8, localized into insulin secretory granules. *Diabetes* 53:2330–2337.
12. Chimienti F, Favier A, Seve M (2005) ZnT-8, a pancreatic beta-cell-specific zinc transporter. *Biometals* 18:313–317.
13. Wenzlau JM, et al. (2007) The cation efflux transporter ZnT8 (Slc30A8) is a major autoantigen in human type 1 diabetes. *Proc Natl Acad Sci USA* 104:17040–17045.
14. Sladek R, et al. (2007) A genome-wide association study identifies novel risk loci for type 2 diabetes. *Nature* 445:881–885.
15. Wenzlau JM, et al. (2008) A common non-synonymous single nucleotide polymorphism in the SLC30A8 gene determines ZnT8 autoantibody specificity in type 1 diabetes. *Diabetes* 57:2693–2697.
16. Saxena R, et al. (2007) Genome-wide association analysis identifies loci for type 2 diabetes and triglyceride levels. *Science* 316:1331–1336.
17. Scott LJ, et al. (2007) A genome-wide association study of type 2 diabetes in Finns detects multiple susceptibility variants. *Science* 316:1341–1345.
18. Zeggini E, et al. (2007) Replication of genome-wide association signals in UK samples reveals risk loci for type 2 diabetes. *Science* 316:1336–1341.
19. Maske H (1957) Interaction between insulin and zinc in the islets of Langerhans. *Diabetes* 6:335–341.
20. Latif ZA, Noel J, Alejandro R (1988) A simple method of staining fresh and cultured islets. *Transplantation* 45:827–830.
21. Shima C, et al. (1996) Enhancement and stabilization of dithizone vital staining for zinc in rat organs using adduct formation. *Anal Biochem* 236:173–175.
22. Qian WJ, Gee KR, Kennedy RT (2003) Imaging of Zn2+ release from pancreatic beta-cells at the level of single exocytotic events. *Anal Chem* 75:3468–3475.
23. Miesenbock G, De Angelis DA, Rothman JE (1998) Visualizing secretion and synaptic transmission with pH-sensitive green fluorescent proteins. *Nature* 394:192–195.
24. Chaurand P, Stoeckli M, Caprioli RM (1999) Direct profiling of proteins in biological tissue sections by MALDI mass spectrometry. *Anal Chem* 71:5263–5270.
25. Bloc A, Cens T, Cruz H, Dunant Y (2000) Zinc-induced changes in ionic currents of clonal rat pancreatic -cells: Activation of ATP-sensitive K+ channels. *J Physiol* 529 Pt 3:723–734.
26. Bancila V, et al. (2005) Two SUR1-specific histidine residues mandatory for zinc-induced activation of the rat KATP channel. *J Biol Chem* 280:8793–8799.
27. Niclauss N, et al. (2008) Computer-assisted digital image analysis to quantify the mass and purity of isolated human islets before transplantation. *Transplantation* 86:1603–1609.
28. Kiekens R, et al. (1992) Differences in glucose recognition by individual rat pancreatic B cells are associated with intercellular differences in glucose-induced biosynthetic activity. *J Clin Invest* 89:117–125.
29. Nicolson TJ, et al. (In press) The type 2 diabetes-associated vesicular zinc transporter *SLC30A8*/ZnT8 is critical for beta-cell Zn^{2+} handling and normal glucose homeostasis. *Diabetes*, in press.
30. Cnop M, et al. (2008) An update on lipotoxic endoplasmic reticulum stress in pancreatic beta-cells. *Biochem Soc Trans* 36:909–915.
31. Scheuner D, et al. (2005) Control of mRNA translation preserves endoplasmic reticulum function in beta cells and maintains glucose homeostasis. *Nat Med* 11:757–764.
32. Pound LD, et al. (2009) Deletion of the mouse Slc30a8 gene encoding zinc transporter-8 results in impaired insulin secretion. *Biochem J* 421:371–376.
33. Ishihara H, et al. (2003) Islet beta-cell secretion determines glucagon release from neighbouring alpha-cells. *Nat Cell Biol* 5:330–335.
34. Louagie E, et al. (2008) Role of furin in granular acidification in the endocrine pancreas: identification of the V-ATPase subunit Ac45 as a candidate substrate. *Proc Natl Acad Sci USA* 105:12319–12324.
35. Ravier MA, Gilon P, Henquin JC (1999) Oscillations of insulin secretion can be triggered by imposed oscillations of cytoplasmic Ca^{2+} or metabolism in normal mouse islets. *Diabetes* 48:2374–2382.
36. Michael DJ, et al. (2004) Fluorescent cargo proteins in pancreatic beta-cells: Design determines secretion kinetics at exocytosis. *Biophys J* 87:L03–L05.
37. Arredouani A, et al. (2002) SERCA3 ablation does not impair insulin secretion but suggests distinct roles of different sarcoendoplasmic reticulum Ca(2+) pumps for Ca(2+) homeostasis in pancreatic beta-cells. *Diabetes* 51:3245–3253.

Supporting Information

Lemaire et al. 10.1073/pnas.0906587106

SI Text

Zinc Transporter Gene Expression Analysis. Total *RNA* from mouse islets was extracted using the Absolutely RNA microprep (Stratagene). Total RNA quantity and quality was determined and RNA profiles of all tested samples were similar with sharp 18S and 28S rRNA peaks on a flat baseline. Total RNA (100 ng) was used to analyze mRNA expression via mouse Gene 1.0 ST arrays according to manufacturer's manual 701880Rev4 (Affymetrix). Briefly, double-stranded cDNA was synthesized with random hexamers tagged with a T7 promoter sequence. Double-stranded cDNA was subsequently amplified by T7 RNA polymerase into antisense cRNA using a Genechip WT synthesis and Amplification kit (Affymetrix). In the second cycle of cDNA synthesis, random hexamers and dUTP were used to prime reverse transcription of cRNA to sense single stranded DNA (ssDNA). Next, cRNA was hydrolyzed and the quality and relative abundance of the ssDNA preparations were assessed. Using uracil DNA glycosylase and apurinic/apyrimidinic endonuclease1, ssDNA (5.5 μg) was fragmented with a GeneChip WT terminal labeling kit (Affymetrix). The fragmented DNA was biotin labeled using Affymetrix DNA Labeling reagent and hybridized to Affymetrix Mouse Gene 1.0 arrays during 17 h at 45 °C in an Affymetrix hybridization oven. Arrays were washed and stained in an Affymetrix fluidics station and scanned using an Affymetrix 3000 GeneScanner. All image files were analyzed using Affymetrix Expression Console™ software and quality controls of the arrays were according to manufacturer's criteria. Raw data were analyzed with RMA sketch using standard settings for Gene 1.0 ST arrays of Expression Console in the AGCC software (Affymetrix).

Vector and Adenovirus Generation. To generate NPY-pHluorin, venus was removed from pNPY-Venus-N1 (kindly provided by A. Miyawaki) by digestion with *Bam*HI and *Not*I. cDNA encoding pHluorin was amplified by PCR from the vector pCI-Vamp2-pHluorin (kindly provided by G. Miesenböck) using the following primers: primer1, 5′- CG*GGATCC*ACGTAGTAAAGGAGAACTTTTCACTGG-3′ (*Bam*HI site underlined); primer 2, 5′-ATTA*GCGGCCGC*TTAACCGGTTTTGTATAG-3′ (*Not*I site underlined), and was then ligated into the same *Bam*HI and *Not*I site of pNPY-Venus-NI. The adenovirus was constructed and amplified, using the pAdEasy system (1). Briefly, NPY-pHluorin plasmid was digested using *Bgl*II and *Not*I and transferred into pShuttle-CMV. Recombination with pAdEasy-1, transfection into HEK 293 cells, and viral amplification were performed as described (1, 2).

Measurements of Pro-Insulin Biosynthesis. Insulin biosynthesis was performed as described earlier, with minor changes (3). Briefly, 15 islets per condition were preincubated for 1h in HEPES Krebs buffer at 5 mM glucose and then labeled with 200 μCi [^{35}S]methionine/cysteine (Perkin-Elmer Easytag express protein labeling mix, specific activity 1,175 Ci/mmol) for 30 min at 37 °C at 10 mM glucose, followed by a 30 min or 1 h chase at 37 °C at 10 mM glucose. The islet lysates were immunoprecipitated using (pro)-insulin antiserum (kindly provided by J. Hutton) and bound to protein A/G Sepharose (GE Healthcare). After elution, newly synthesized pro-insulin and insulin were separated by SDS/PAGE and quantified for autoradiographic signals using Scion Image densitometry software.

Static Insulin Release. Insulin release was measured from statically incubated, size matched, freshly isolated islets (n = 7 per tube). Incubations were for 1 h at 37 °C in HEPES-buffered Krebs solution (+ 0.5% BSA), supplemented with 5 mM, 10 mM or 20 mM glucose. After incubation of the islets, the supernatant was removed immediately and frozen for insulin release measurement, using a commercially availabe ELISA kit (Mercodia). The islet pellets were resuspended in ice-cold acid-EtOH (75% EtOH, 0.1 N HCl) to measure insulin content.

1. He TC, et al. (1998) A simplified system for generating recombinant adenoviruses. *Proc Natl Acad Sci USA* 95:2509–2514.
2. Ravier MA, Rutter GA (2005) Glucose or insulin, but not zinc ions, inhibit glucagon secretion from mouse pancreatic alpha-cells. *Diabetes* 54:1789–1797.
3. Scheuner D, et al. (2005) Control of mRNA translation preserves endoplasmic reticulum function in beta cells and maintains glucose homeostasis. *Nat Med* 11:757–764.

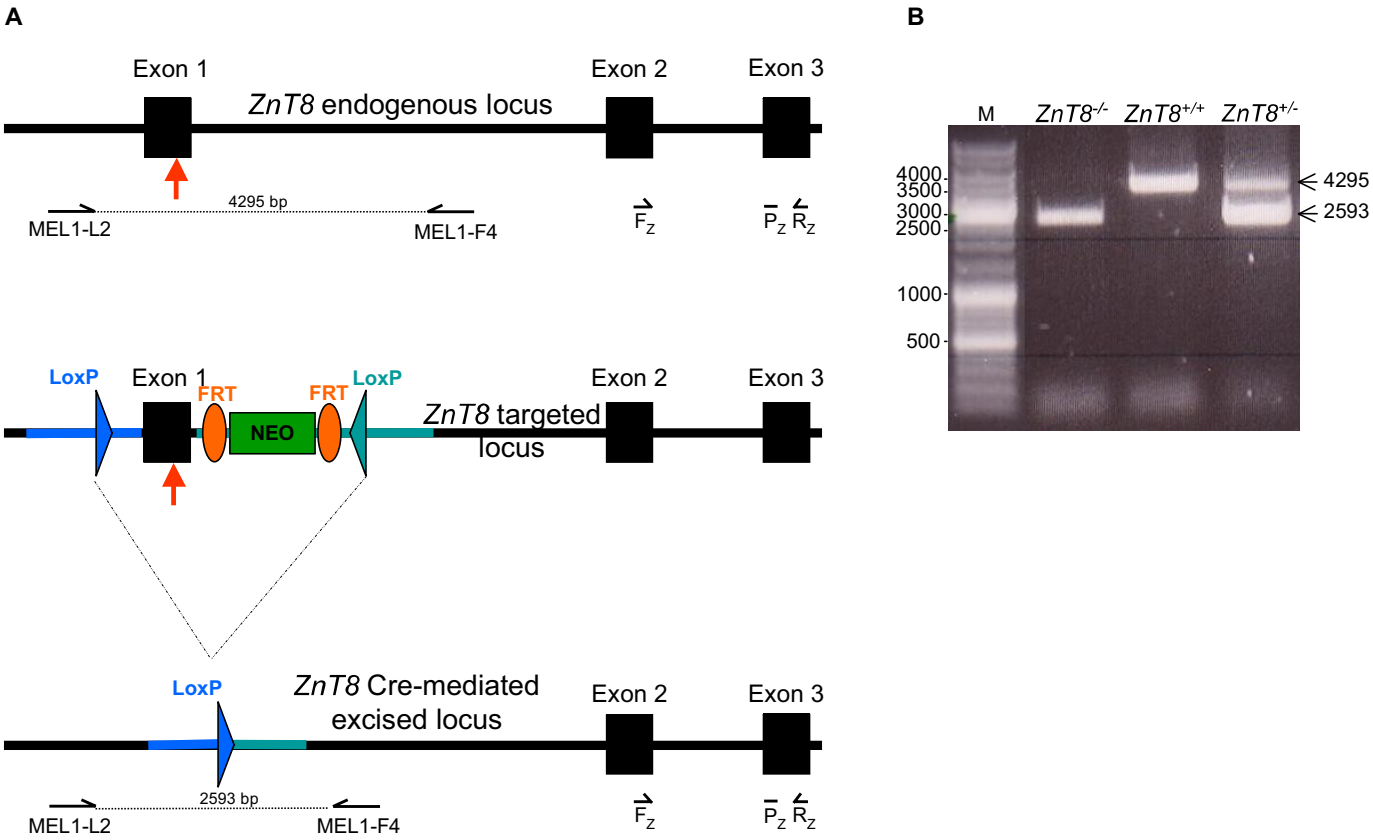

Fig. S1. ZnT8 knock out strategy. (*A*) ZnT8 knockout mice were generated by insertion of a *Lox*P site together with an FRT flanked neomycin selection cassette within intron 1 and a proximal *Lox*P site within the upstream exon 1, resulting in a recombination event that removes control elements of transcription and the start codon for translation (red arrow). MEL1-L2 and MEL1-F4 are the primers used for genotyping. F_z, P_z adn R_z are the primers used for QPCR. (*B*) PCR examples of genotyping of $ZnT8^{-/-}$, $ZnT8^{+/+}$ and $ZnT8^{+/-}$ mice. M, marker.

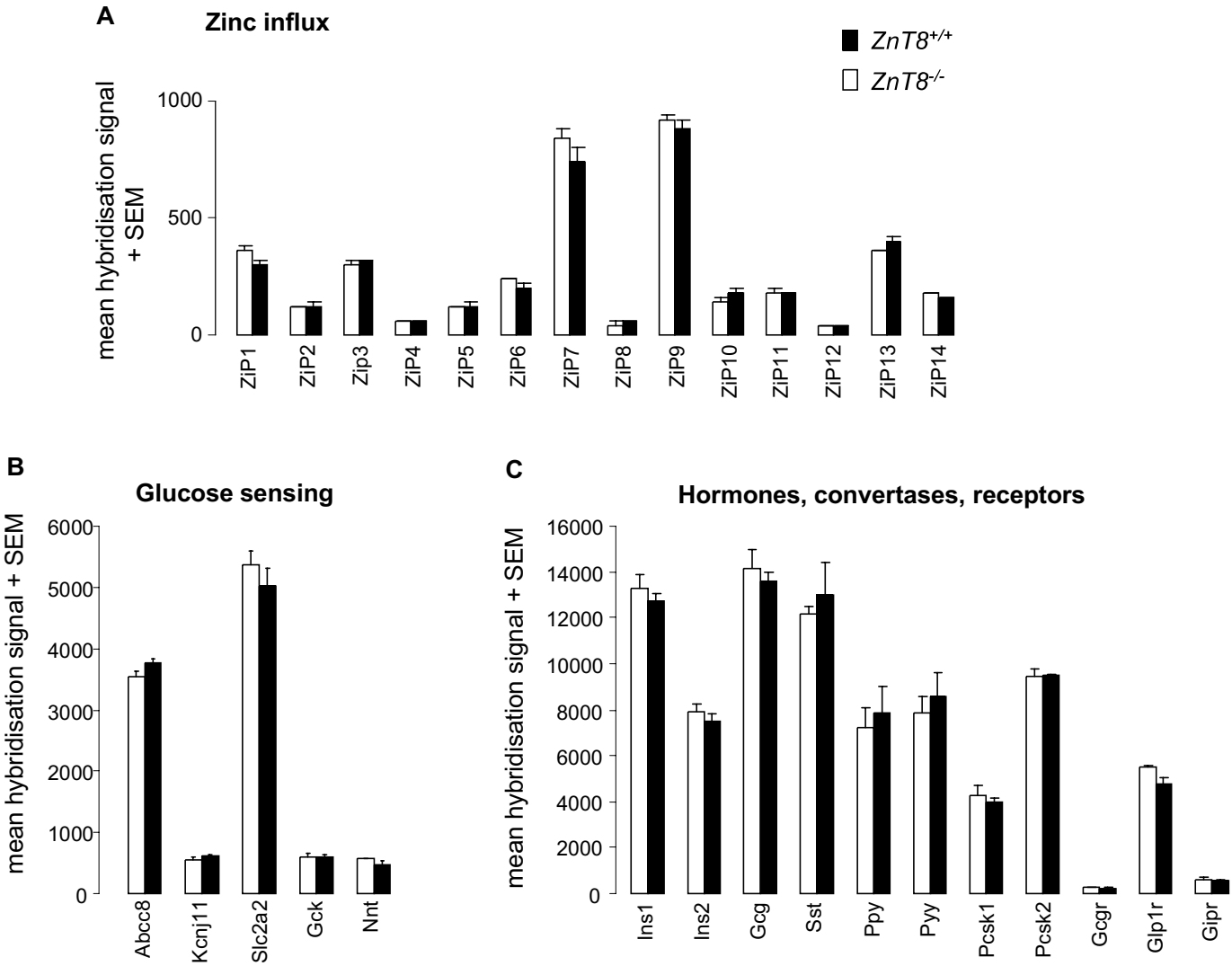

Fig. S2. microarray analysis of islets from *ZnT8*$^{-/-}$and *ZnT8*$^{+/+}$ mice. mRNA expression of (*A*) the 14 known influx zinc transporters (ZiP), (*B*) genes involved in glucose sensing, and (*C*) hormones, prohormone convertases and incretin hormone receptors.

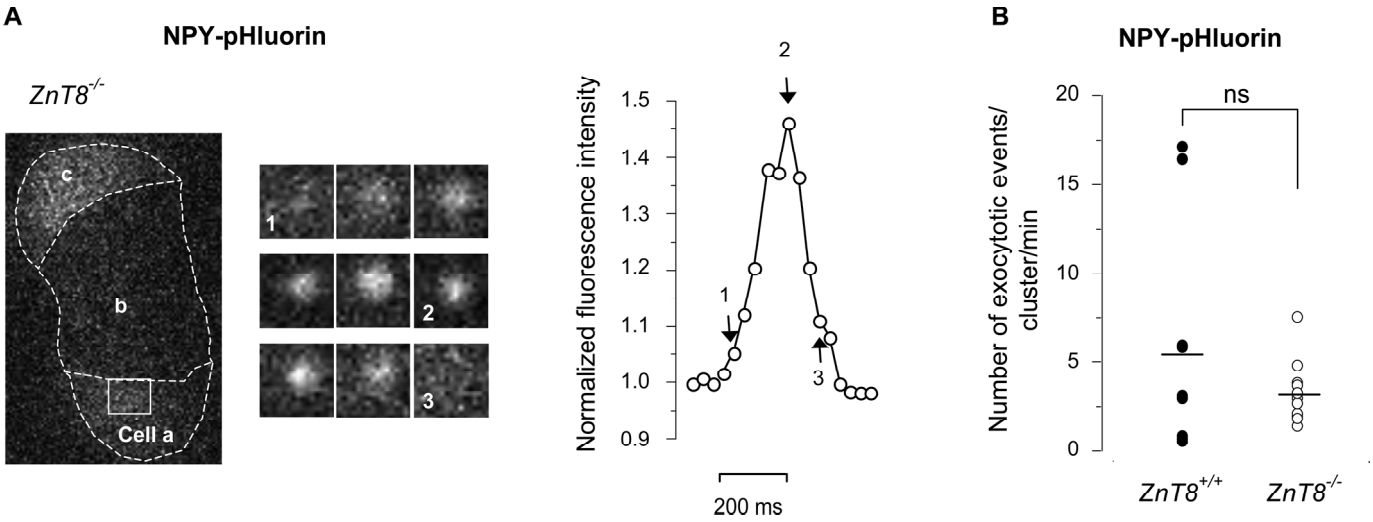

Fig. S3. Exocytosis in islets from $ZnT8^{-/-}$and $ZnT8^{+/+}$ beta cells. (*A*) Insulin exocytosis stimulated by 15 mM glucose and 1 μM forskolin was imaged during 7 min by total internal reflection fluorescence microscopy after adenoviral expression of NPY-pHluorin. One representative exocytosis event from a cell within a $ZnT8^{-/-}$ three-cell cluster is illustrated. Delimitation between cells is shown by dotted lines on the left panel, single images taken every 30 ms in the region delimited by a square from ''cell a'' are illustrated in the middle, and the intensity of fluorescence for this release event is plotted on the right panel. Arrows show fluorescence intensity for the indicated time points illustrated in the middle panel. (*B*) Number of flashes counted manually in clusters of $ZnT8^{+/+}$ and $ZnT8^{-/-}$ islet cells in similar experiments as that illustrated in *A*. The horizontal line shows the average of 12 clusters from three individual mice.

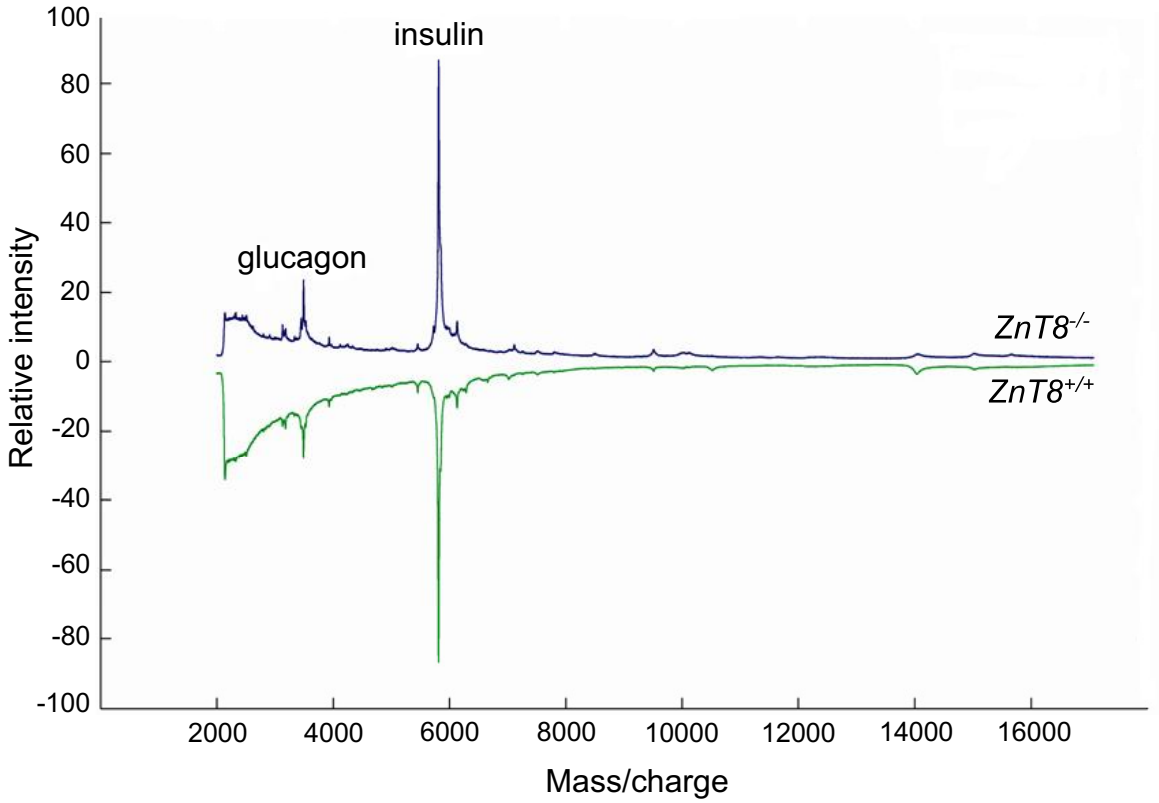

Fig. S4. Normal insulin and glucagon profile in *ZnT8*$^{-/-}$ mice. Comparison of mass spectral tissue profiling signatures of beta cells in pancreatic sections from *ZnT8*$^{-/-}$ and *ZnT8*$^{+/+}$ mice. Collected average beta cell profiles are mirrored to facilitate visual comparison. Insulin and glucagon masses (5,800 and 3,483 Da, respectively) are indicated.

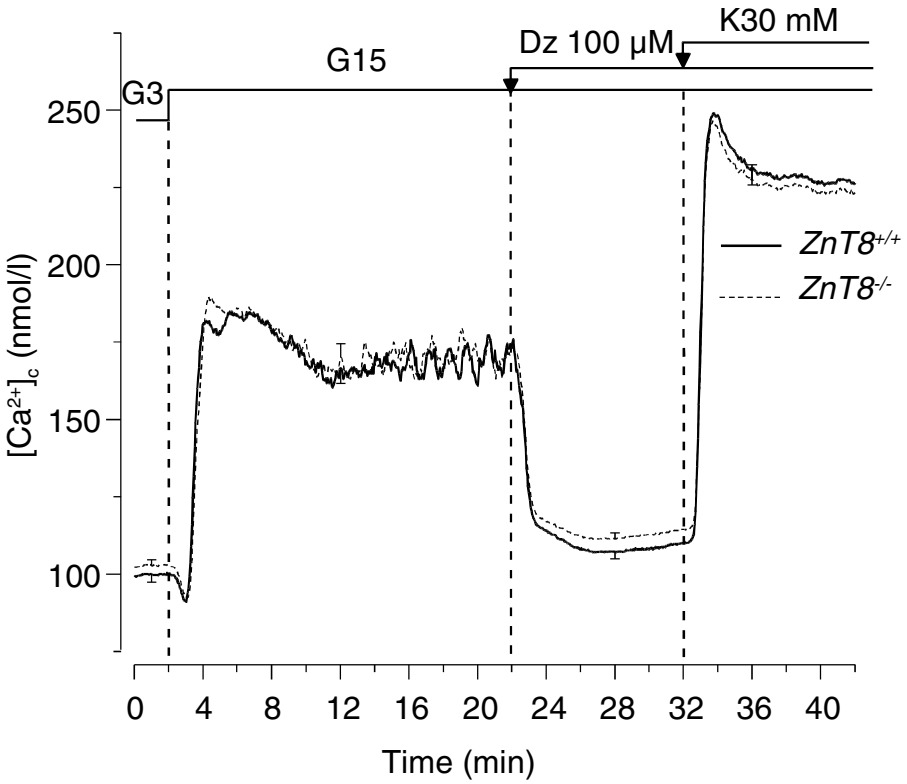

Fig. S5. Changes in free cytosolic calcium concentration are normal in *ZnT8*$^{-/-}$ mice. After overnight culture in 10 mM glucose (G), islets from adult *ZnT8*$^{+/+}$ (solid line) and *ZnT8*$^{-/-}$ (dotted line) mice were perifused for 30 min with a medium containing 3 mM glucose. Only the last period of perifusion in G3 is shown. When indicated by the arrows, the glucose concentration was increased to 15 mM, the K_{ATP} channel opener diazoxide (Dz) was added, and the KCl concentration was increased from 4.8 to 30 mM. Data are mean ± SEM of 35 *ZnT8*$^{+/+}$ and 42 *ZnT8*$^{-/-}$ islets.

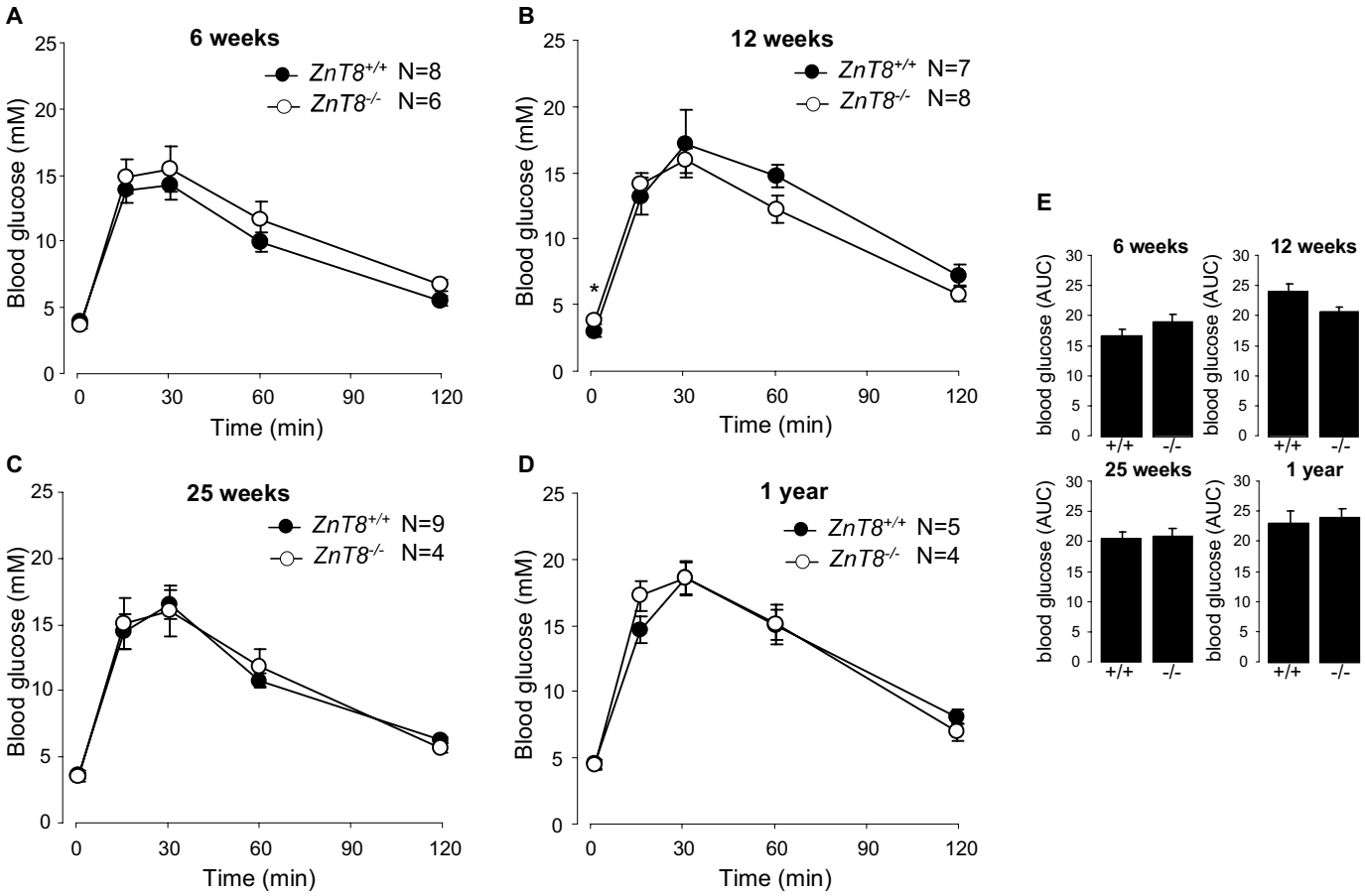

Fig. S6. Intraperitoneal glucose tolerance of male $ZnT8^{-/-}$ and $ZnT8^{+/+}$ mice. Blood glucose levels were measured at the indicated time points after i.p. injection of 2.5 mg glucose/g BW glucose in overnight (16 h) fasted mice aged 6 weeks (*A*), 12 weeks (*B*), 25 weeks (*C*), and 1 year (*D*), (*E*) Results of *A*–*D* calculated as area under the curve (AUC). $ZnT8^{+/+}$ (black circles) and $ZnT8^{-/-}$ (open circles), data are mean ± SEM with N per strain and age as indicated. Statistical significances of differences between $ZnT8^{+/+}$ and $ZnT8^{-/-}$ mice were calculated with the unpaired Student's *t* test: , $P \leq 0.05$.

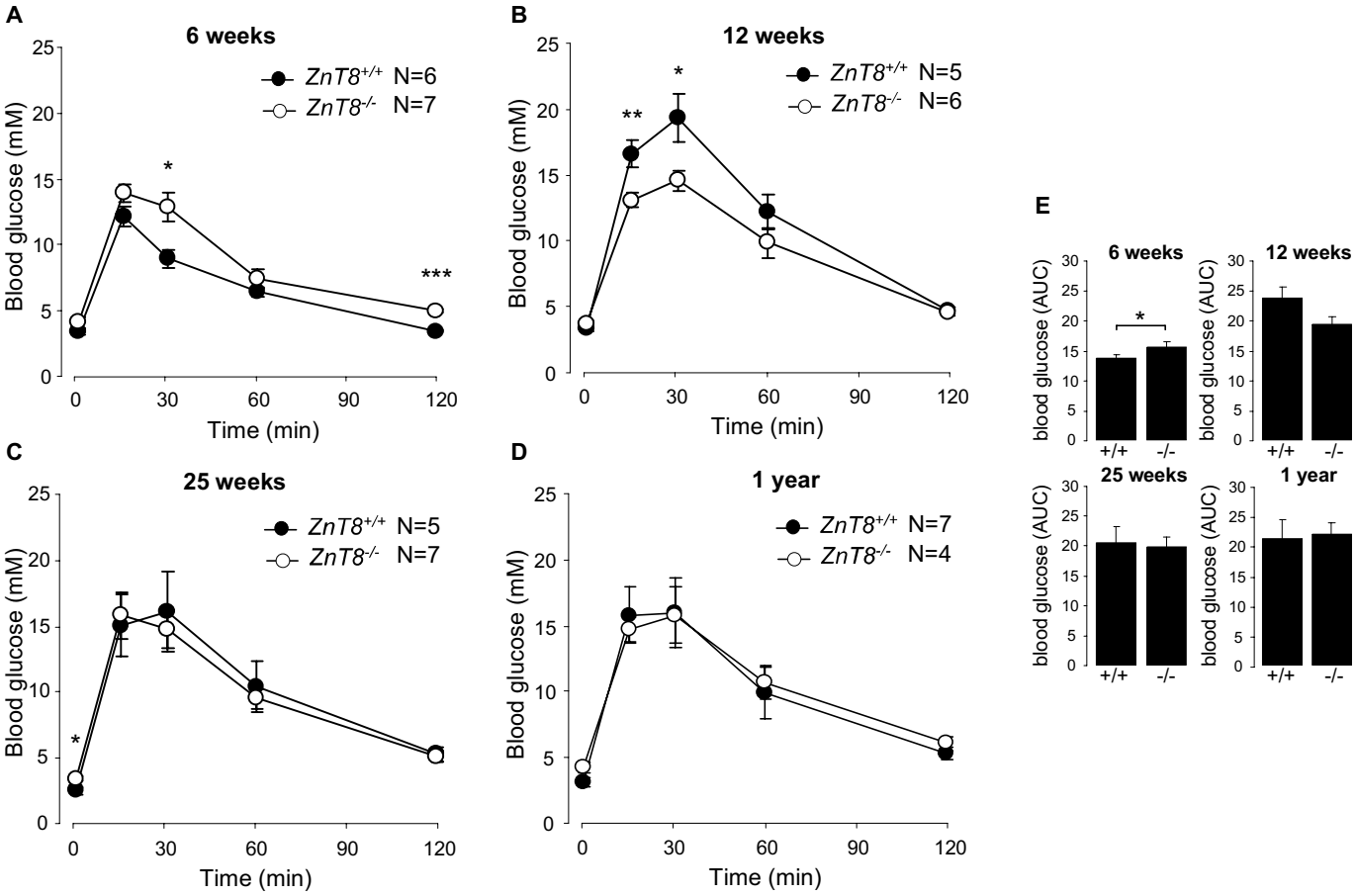

Fig. S7. Intraperitoneal glucose tolerance of female $ZnT8^{-/-}$ and $ZnT8^{+/+}$ mice. Blood glucose levels were measured at the indicated time points after i.p. injection of 2.5 mg glucose/g BW glucose in overnight (16 h) fasted mice aged 6 weeks (*A*), 12 weeks (*B*), 25 weeks (*C*), and 1 year (*D*), E. Results of *A*–*D* calculated as area under the curve (AUC). Data are mean ± SEM with N per strain and age as indicated. Statistical significances of differences between $ZnT8^{+/+}$ (black circles) and $ZnT8^{-/-}$ (open circles) mice were calculated with the unpaired Student's *t* test: , $P \leq 0.05$; , $P \leq 0.005$.

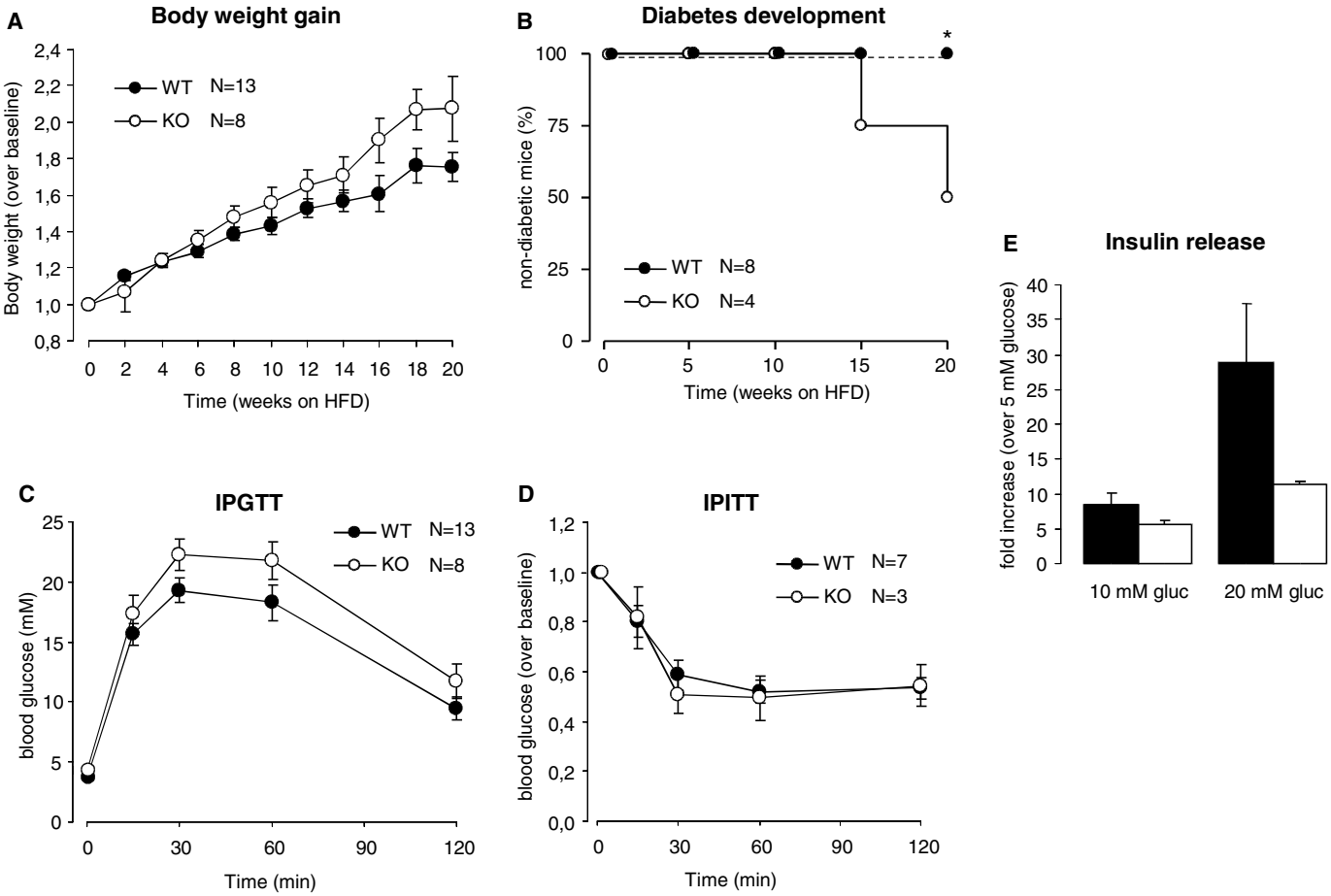

Fig. S8. Characterization of $ZnT8^{+/+}$ and $ZnT8^{-/-}$ mice fed a high fat diet for several weeks. $ZnT8^{+/+}$ (black circles) and $ZnT8^{-/-}$ (open circles) male mice were given a high fat diet from the age of 6 weeks. (*A*) Body weight was measured every 2 weeks, (*B*) Time course of the percentage of animals of the $ZnT8^{+/+}$ and $ZnT8^{-/-}$ strains that did not develop diabetes (blood glucose levels <14 mM) after feeding a HFD. At the end of the observation period the difference between $ZnT8^{+/+}$ and $ZnT8^{-/-}$ mice was significant (χ^2 test $P = 0.028$). (*C*) Intraperitoneal glucose tolerance after 10 weeks on HFD, (*D*) i.p. insulin tolerance test after 16 weeks on HFD, E. static insulin release on isolated islets, incubated with 5 mM, 10 mM and 20 mM glucose for 1 h. Data (mean ± SEM, $n = 3$) are expressed as fold change over basal release measured at 5 mM glucose.

Table S1. Blood glucose levels in ZnT8$^{+/+}$ and ZnT8$^{-/-}$ mice of 12 and 25 weeks old

	ZnT8$^{+/+}$		ZnT8$^{-/-}$	
	12 weeks	25 weeks	12 weeks	25 weeks
All				
Blood glucose, mM	6.44 ± 0.17	6.74 ± 0.28	6.40 ± 0.26	6.43 ± 0.24
n	26	16	31	15
Fasted blood glucose, mM	3.31 ± 0.24	3.12 ± 0.25	3.73 ± 0.15	3.34 ± 0.18
n	14	14	14	11
Male				
Blood glucose, mM	6.59 ± 0.20	7.33 ± 0.37	6.50 ± 0.39	7.12 ± 0.26
n	19	9	19	7
Fasted blood glucose, mM	3.32 ± 0.35	3.51 ± 0.29	3.78 ± 0.18	3.43 ± 0.41
n	9	9	8	4
Female				
Blood glucose, mM	6.03 ± 0.28	5.98 ± 0.22	6.25 ± 0.31	5.83 ± 0.23
n	7	7	12	8
Fasted blood glucose, mM	3.28 ± 0.29	2.11 ± 0.07	3.65 ± 0.28	3.29 ± 0.20
n	5	5	6	7*

Data are means ± SEM. *, $P < 0.05$.

Table S2. Insulin and glucagon levels in male ZnT8$^{+/+}$ and ZnT8$^{-/-}$ mice

	ZnT8$^{+/+}$	ZnT8$^{-/-}$
Plasma insulin, ng/mL	0.78 ± 0.21	0.76 ± 0.18
n	10	13
Plasma glucagon, pg/mL	47 ± 3.51	66 ± 10.59
n	7	5

Data are means ± SEM, average age 12 weeks, insulin and 23 weeks, glucagon